INTERNATIONAL JOURNAL OF AUTOMOTIVE AND MECHANICAL ENGINEERING
ISSN: 2229-8649 e-ISSN: 2180-1606
VOLUME 23, ISSUE 1, 2026, 13321 - 13338
DOI: https://doi.org/10.15282/ijame.23.1.2026.12.1010

RESEARCH ARTICLE

Topology optimization of the front steering knuckle structure of a formula SAE racing car

Agustin Ramirez[1], Christian E. Yactayo[1], Christian V. Rodriguez[1*], and Dennys De La Torre[2]

[1]Universidad Tecnológica del Perú, 15046 Lima, Perú
[2]Universidad Nacional de Ingeniería, Av. Túpac Amaru 210 – Lima, Perú

Abstract – The Formula SAE (FSAE) competition is an international student event that seeks to design a lightweight single-seater to maximize performance. In this context, the front steering knuckle represents a significant challenge, as its weight directly influences the vehicle's dynamic performance. However, previous studies have limitations regarding the combined use of topology optimization tools and the evaluation of new materials for this component. This research addresses this gap by topologically optimizing the front steering knuckle of an FSAE single-seater to reduce its weight while maintaining its structural strength. Initially, the stresses at the knuckle's support points were calculated, considering Formula SAE regulations and the vehicle's operational conditions (acceleration, braking, cornering, and overcoming obstacles). The knuckle was modeled in SolidWorks, and its structural parameters (stress, deformation, and factor of safety) were analyzed in ANSYS using lightweight and durable materials such as Aluminum 7075-T6 and Alumold, the latter being analyzed for the first time in this context. Finite element analysis was performed, and a suitable mesh was selected from six options. Subsequently, topology optimization was applied to remove unnecessary material using ANSYS and SolidWorks software, reducing the initial knuckle mass of 2.41 kg by 35% and 25%, respectively, while maintaining a minimum factor of safety of 1.5. This approach demonstrates the effectiveness of topology optimization in enhancing the structural design of automotive components.

Article History
Received : 20 March 2025
Revised : 04 August 2025
Accepted : 28 January 2026
Published : 12 March 2026

Keywords
Formula SAE
Front steering knuckle
Finite element analysis
Topology optimization
Racing car
Structural design

1. Introduction

The Formula SAE (FSAE) [1] is an international engineering competition that challenges university students to design, build, and compete with Formula single-seater vehicles. These vehicles undergo various loads during the competition's static and dynamic events. Within the vehicles, the front steering knuckle plays a critical role by connecting the suspension components and wheels, ensuring stability and performance during driving. Previous research has been conducted on the front steering knuckles of various vehicles. For instance, Kaldhone and Sapkal [2] re-engineered a front steering knuckle using Finite Element Analysis (FEA) and Topology Optimization (TO) to maximize stiffness and reduce weight. Using Cr-Ni steel, they achieved a 35.58% reduction in weight without compromising structural strength. Dumbre et al. [3] optimized a front steering knuckle using FEA and topology optimization to reduce weight while maintaining strength and rigidity. The front steering knuckle was modelled in CATIA, with HyperWorks and OptiStruct used for structural analysis and optimization, respectively, resulting in an 11% weight reduction. Additionally, Kim et al. [4] reduced the weight of a front steering knuckle using the kriging method, achieving a 60% reduction by switching from GCD45 (cast steel) to Al6082M. Anitha and Shankar [5] applied shape and topology optimization techniques to reduce the weight of the front steering knuckle, evaluating materials such as cast iron, aluminum, and S-glass epoxy. Using Creo Parametric for modelling and ANSYS for structural analysis, they reduced the mass to 0.8755 kg and 0.6321 kg for aluminum and S-glass epoxy, respectively, with maximum stresses of 53.81 MPa and 76.12 MPa. These studies demonstrate that front steering knuckle optimization through FEA and TO improves weight efficiency while maintaining strength within safety limits. It is important to note that TO is a method that redistributes material within a given design space to meet strength constraints while minimizing mass.

Other competition vehicles, such as All-Terrain Vehicles, have also been studied. Haisundaram et al. [6] redesigned an ATV front steering knuckle to reduce weight using cast iron, achieving a 17.53% reduction while maintaining a satisfactory Factor of Safety (FoS). Similarly, Bhusari et al. [7] optimized an ATV front steering knuckle using EN24 alloy steel, achieving a 62.78% weight reduction with a maximum stress of 327 MPa and a FoS of 2.05. Bhardwaj et al. [8] optimized an ATV front steering knuckle using Al7075-T6 alloy, achieving an 18% weight reduction and a 36% increase in FoS while maintaining rigidity and strength. Dusane et al. [9] analyzed an ATV front steering knuckle with an initial mass of 60 kg, applying forces of 1400 N, 2800 N, and 4000 N in the x, y, and z directions, respectively. Their modified design, analyzed in CATIA and ANSYS, showed a maximum stress of 72.394 MPa and reduced stress under assigned loads. Rajeshkumar et al. [10] improved the ATV suspension and steering using SolidWorks and ANSYS, optimizing wheel assembly mass without affecting geometric and load-transfer characteristics. Shuaib et al. [11] minimized front steering knuckle weight by considering weight reduction, design constraints, and variables, achieving reduced stress concentration and improved performance. Note that commonly only one software is used to carry out TO, and there is no comparative analysis between the results of TO with SolidWorks and ANSYS software, to the authors' knowledge.

*CORRESPONDING AUTHOR | Christian V. Rodriguez | ✉ C25183@utp.edu.pe

For the FSAE racing car, Saputro et al. [12] determined the structural parameters of an FSAE car front steering knuckle using static load simulations. They used AISI 1018 mild steel, with Fusion 360 for design and simulation, resulting in a maximum deformation of 0.01281 mm, a stress of 370 MPa, and an FoS of 5.24. Yadav et al. [13] optimized a front steering knuckle using cast iron and mild steel, achieving a 5.64% mass reduction with EN47 forged steel. Li et al. [14] reduced the weight of a front steering knuckle for an electric Formula car using TO, achieving a 60% mass reduction with Al7075. Gupta et al. [15] designed and analyzed a front steering knuckle using Al6061-T6, achieving an 11% weight reduction. Agarwal and Saatyaki [16] conducted fatigue analysis on FSAE front steering knuckles, estimating a lifespan of 180,000 cycles. Hasan et al. [17] designed and analyzed a front steering knuckle using TO, achieving a 39.28% weight reduction with 4130 steel. Kothari et al. [18] optimized FSAE front steering knuckles using Al6061-T6, maintaining an FoS above 1 under dynamic loads. Mesicek et al. [19] topologically optimized an FSAE connecting rod using 3D printing with Inconel 718, achieving a 7% mass reduction and a 32% increase in stiffness. Pang and Fard [20] used reverse engineering and topology optimization to reduce the weight of a crank mechanism, achieving a 16.5% reduction in maximum Von-Mises stress. Wable and Shah [21] optimized an FSAE front steering knuckle using Al6061 and Al7075, achieving a 20% weight reduction. The literature presents a lack of studies involving novel materials such as Alumold in FSAE vehicle parts. The research problem addressed in this paper is the need to reduce the weight of the front steering knuckle in a Formula SAE racing car while maintaining its structural strength and performance under the demanding conditions of the competition. As indicated in the scientific literature, reducing front steering knuckle weight improves vehicle performance by enhancing acceleration, maneuverability, and stability. To ensure functionality, the front steering knuckle must withstand stresses during demanding conditions such as acceleration, braking, and cornering. This is achieved by analyzing loads at the front steering knuckle's contact points, ensuring the design does not compromise safety or performance.

Therefore, the primary objective of this work is to optimize the design of the front steering knuckle for a Formula SAE racing car to achieve significant weight reduction without compromising structural integrity or performance. Initial calculations of stresses at the front steering knuckle's anchor points are performed, considering vehicle components. The front steering knuckle is designed and modelled using SolidWorks. The TO is applied using ANSYS and SolidWorks, with a threshold FoS of 1.5. Materials used are Al7075-T6 and Alumold. Structural analysis in ANSYS determines the best material, reducing mass, stress concentration, and deformation while maintaining the required FoS. This paper makes three principal contributions to the structural optimization of vehicle components. First, it presents a case study on the TO of the front steering knuckle for a Formula SAE racing car, achieving a design that reduces weight while enhancing suspension performance. Second, it provides a functional comparison by employing two distinct software tools (ANSYS and SolidWorks) for the TO process, thereby offering practical insights into their application. Third, it expands the material selection analysis by evaluating two aluminum alloys, Al7075-T6 and Alumold, with the latter being investigated for the first time within this specific automotive structural context.

2. Materials and Methods

2.1 Calculation of Stresses at the Anchoring Points of the front Steering Knuckle

To find the acceleration, total front tire braking force, total vertical load, and braking torque, we use Figure 1, which shows the reactions and forces on the tires.

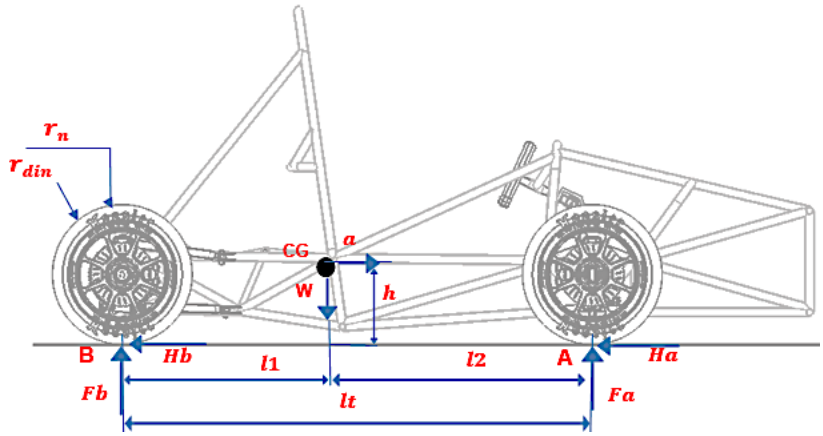

Figure 1. Side view of the vehicle showing friction and reaction forces on tires

The equation of the acceleration, a, is:

$$a = \frac{v_f - v_i}{t} \tag{1}$$

where v_f is the final velocity, v_i is the initial velocity, and t is the time. The parameters follow the FSAE 2024 regulations [22].

Longitudinal mass transfer occurs when the vehicle brakes, accelerates, or navigates a curve. This increases the normal reaction force on the front tires, resulting in the greatest mass transfer. The equation for the total braking force of the front tire, ΔF_a, is

$$\Delta F_a = \frac{a \cdot m \cdot h}{lt} \quad (2)$$

where m is the combined mass of the vehicle plus the driver, h is the vertical distance from the vehicle's gravity centre to the ground, and lt is the distance between axes.

The total vertical load equation, C_{vt}, uses the weight of the vehicle together with that of the driver (W) plus ΔFa during braking.

$$C_{vt} = W + \Delta F_a \quad (3)$$

where W is the combined mass of the vehicle plus the driver.

Figure 1 illustrates the reaction and friction forces at points A and B (F_a, F_b, H_a, and H_b). The equations to quantify them are presented as follows. The equation of the tire inertia moment, I_n, is

$$I_n = k * m_n * (r_n)^2 \quad (4)$$

where k is the tire mass distribution product, m_n is the tire mass, and r_n is the actual tire radius.

The equation of the normal force at point B, F_b, considers I_n, m, a, h, lt, dynamic radius (r_{din}), friction coefficient (μ), gravitational acceleration (g), and the distance to the front axle (l_2) (y-direction).

$$F_b = \frac{\left(\frac{4 \cdot I_n \cdot \mu}{r_{din}}\right) - m \cdot (a \cdot h + g \cdot l_2)}{lt} \quad (5)$$

The equation of the normal force at point A, F_a, considers W (y-direction) y F_b.

$$F_a = W - F_b \quad (6)$$

The friction force at point A, H_a, is given by the equation:

$$H_a = F_a \cdot \mu \quad (7)$$

The friction force at point B, H_b, is

$$H_b = (m \cdot a) \cdot H_a \quad (8)$$

The braking moment on the front steering knuckle at point A, M_f, is

$$M_f = \frac{H_a}{2} \cdot r_{din} \quad (9)$$

When the vehicle takes a curve and turns, centrifugal force, $F_{centrifugal}$, (due to centrifugal acceleration, $A_{centrifugal}$) acts on the tires. Part of these loads is absorbed by the suspension. To calculate $F_{centrifugal}$, data from the autocross event are used, where an average velocity, v_x, of 40 to 48 km/h is considered. Additionally, the diameter of FSAE competition tracks ranges between 23 and 45 m [23]. Figure 2 illustrates a vehicle on a curve.

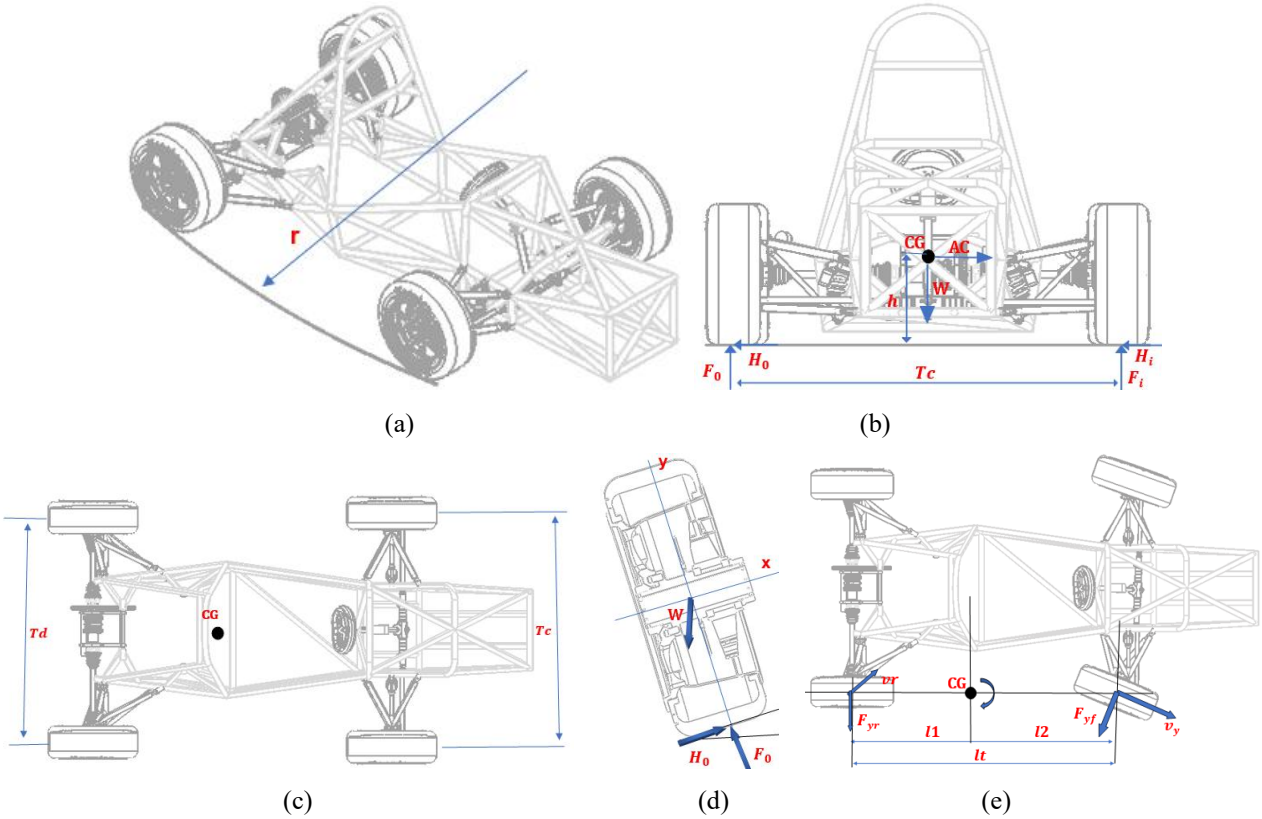

Figure 2. Free body diagram of the racing car on a curve: (a) isometric view, (b) front view, (c) front and back width of the car from top view, (d) turn in a curve, and (e) top view

The $F_{centrifugal}$, and $A_{centrifugal}$ equations are

$$F_{centrifugal} = \frac{m \cdot {v_x}^2}{r} \tag{10}$$

where v_x is the velocity in x, and r is the curve radius.

$$A_{centrifugal} = \frac{F_{centrifugal}}{m} \tag{11}$$

The vertical normal load is then denoted, F_0,

$$F_0 = \frac{W}{2} + \frac{F_{centrifugal} \cdot h}{T_c} \tag{12}$$

The equation calculates the increase in load on the front tires caused by changes in cornering momentum, since the greater the vertical load, the lower the coefficient of friction, giving the tire better grip on the surface, where T_c is the front width of the car, as shown in Figure 2(c). To determine the front tire lateral load in cornering, H_0, Newton's second law is applied. Figure 2(d) shows the free-body diagram of the tyre during cornering, highlighting the forces acting on the contact patch. The H_0 equation is

$$H_0 = m \cdot A_{centrifugal} + (F_0 - W) \cdot \sin\theta \tag{13}$$

When the driver turns the steering wheel of the racing car to navigate a curve, a lateral force is generated in the steering system. This force is transmitted through the steering rod to the knuckle and then to the tires, enabling the front axle to turn. It is assumed that the vehicle is moving at a speed, v_1, of 40 km/h, with a minimum diameter of 9 m for tight curves on the circuit, as per FSAE regulations [22]. Figure 2(e) illustrates the lateral force on the front axle, F_{yf}, of a cornering vehicle.

The F_{yf} equation is

$$F_{yf} = m \cdot \frac{(v_1)^2}{r_1} * \frac{l_2}{lt} \tag{14}$$

where v_1 is the vehicle speed, and r_1 is the curvature radius.
Figure 3 shows the steering joint subject to F_{yf} which occurs on the cornering vehicle.

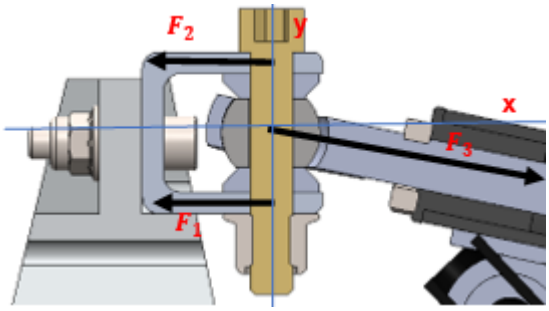

Figure 3. Double shear force in the steering joint

The bolt shear stress, τ_p, is the force parallel to its cross-sectional area divided by the area that the bolt tries to cut, and its formula is expressed as Eq. (15).

$$\tau_p = \frac{H_0}{2\pi * \left(\frac{\emptyset}{2}\right)^2} \tag{15}$$

where ϕ is the bolt diameter.
The shear stress at point C refers to the shear stress at a given point of a bolt or other element, and its formula is

$$\tau_c = \frac{H_0}{4 * S_r * e} \tag{16}$$

where S_r is the resistant section, e is the thickness.

When the vehicle travels on an FSAE circuit and passes over an obstacle on the track, a vertical acceleration is generated. This acceleration is determined by considering the following parameters: constant speed of 48 km/h, triangular-shaped obstacle with a 30° slope, maximum height of 10 cm, with the tires maintaining contact with the surface [23]. Figure 4 shows the free-body diagram of the vehicle as it overcomes the obstacle.
The vertical velocity equation, v_y, is

$$v_y = v_x * \tan(\beta) \tag{17}$$

where v_x is the horizontal velocity, as shown in Figure 4, and β is the obstacle slope.

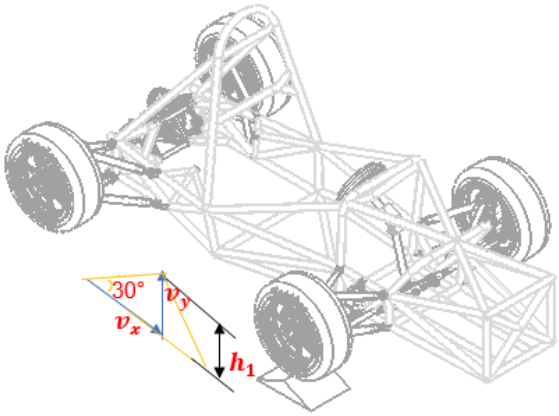

Figure 4. Free body diagram of the vehicle passing through an obstacle

When the vehicle passes over a track obstacle, a vertical acceleration is generated along the y-axis, a_y.

$$a_y = \frac{v_y^2 - v_{y2}^2}{2 \cdot h_1} \tag{18}$$

where v_{y2} is the vehicle's final speed, h_1 is the obstacle height.

The force exerted on the tires arises from the vehicle's mass transfer. This assumes a weight distribution of 60% on the front axle and 40% on the rear axle [23]. The expression is obtained as follows.

$$F_{on\_tires} = \frac{R_{rd}}{100} * m * a_y \tag{19}$$

for the force on tires when overcoming an obstacle, where R_{rd} is the mass distribution corresponding to the front wheels.

2.2 Design of the Front Steering Knuckle

The components involved in the design of the front knuckle are described. The design process is not carried out in isolation from the systems it interacts with, as the characteristics of these components can impose geometric constraints on others. These constraints may influence the final design. Below, the most important components to be considered in the design are described. The steering rack is responsible for orienting the steering tires, enabling the FSAE vehicle to be maneuverer within the competition track. Table 1 shows the Kaz Technologies steering rack specifications, which are one of the representatives used in FSAE. Tyres are essential in FSAE competitions, as they directly impact the vehicle's performance in terms of traction, handling, acceleration, and braking. Table 2 shows the Hoosier Racing Tyres specifications, a representative brand in FSAE. These tires were selected because they provide maximum grip, stability, and control under various dry or wet track conditions. The rim dimensions commonly used in FSAE competition are 10" and 13". Table 3 shows the OZ Formula Student Magnesium CL 13" rim dimensions, which provide greater interior space and are commonly used for first-year teams in FSAE competition.

Table 1. Steering rack specifications (Kaz Technologies) [24]

Description	Unit	Magnitude
Weight	kg	1.36
Maximum distance	mm	82.55
Pinion rotation	degrees	248

Table 2. Tire specifications (Hoosier Tire: 20.5x7.0 -13 R20) [25]

Nomenclature	Description	Unit	Magnitude
D_n	Tire diameter	mm	520.7
m_n	Tire mass	kg	5
k	Tire mass distribution ratio	-	0.75
μ_y	Coefficient of lateral friction	-	1.6
μ_x	Coefficient of longitudinal friction	-	1.7

The brake disc is a critical component of the vehicle's brake system. Its primary function is to provide the surface on which the brake pads act to reduce speed or stop the vehicle. Table 4 shows the NG Brakes brake disc features, which have a mass of 0.9 kg, compared to other heavier discs with inferior heat dissipation. The brake calliper is fixed to the front steering knuckles. It features two or three pairs of pistons, evenly distributed on both sides of the calliper. Table 5 shows the Wilwood GP200 calliper characteristics. This calliper includes two pistons with a diameter of 31.75 mm and a

mass of 0.41 kg. The wheel hub is commonly used to provide a stable rotation point for the wheel and brake disc, enabling the braking torque from the disc to be transmitted to the tire. Additionally, the wheel hub secures the bearing and supports the load generated when the vehicle navigates an FSAE competition curve. Figure 5 shows the design of the wheel hub, which has a mass of 0.952 kg and is made of 7075-T6 aluminum [29]. The bearing allows the wheel centre to rotate freely with the tyre, while the front steering knuckle remains fixed in its vertical position. The selection of bearings is based on axial loads, maximum rotational speed, and the available space in the front steering knuckle. Table 6 shows the SKF 61913 deep groove ball bearings specifications, chosen for their ability to withstand significant axial forces in both longitudinal and transverse directions. These forces occur during driving in FSAE competitions.

Table 3. Rim specifications (OZ Racing) [26]

Nomenclature	Description	Unit	Magnitude
D_r	Hoop diameter	mm	330.2
m_r	Mass of the hoop	kg	2.45

Table 4. Brake disc specifications (NG) [27]

Nomenclature	Description	Unit	Magnitude
D_{ed}	Outer diameter of the disc	mm	220
D_{id}	Inner diameter of the disc	mm	122
t_d	Disc thickness	mm	4

Table 5. Wilwood GP200 Calliper Specifications [28]

Description	Unit	Magnitude
Support center	mm	60.9
Free support space	mm	21.8
Mounting hole diameter	mm	8.1

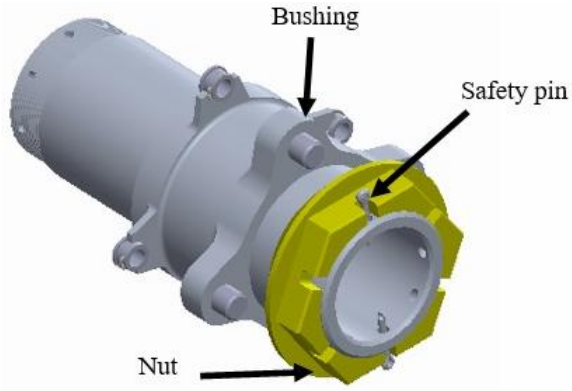

Figure 5. Wheel hub assembly

Table 6. Deep groove ball bearing specifications (SKF) [30]

Description	Unit	Magnitude
Internal diameter	mm	65
External diameter	mm	90
Width	mm	13
Basic dynamic load capacity	kN	17.4
Basic static load capacity	kN	13.4
Rotational speed reference	rpm	15000
Rotational speed limit	rpm	9500

2.3 Three-Dimensional Modelling

Figure 6(a) shows the anchor points and suspension geometry to model the front steering knuckle, considering the four angles: camber, caster, kingpin, and opening (convergence and divergence). Figure 6(b) shows the geometry of the front suspension. Figure 6(c) illustrates the base geometry for the design of the front steering knuckle, considering the dimensions of the components. Figure 6(d) displays the initial sketch of the front steering knuckle body's geometry.

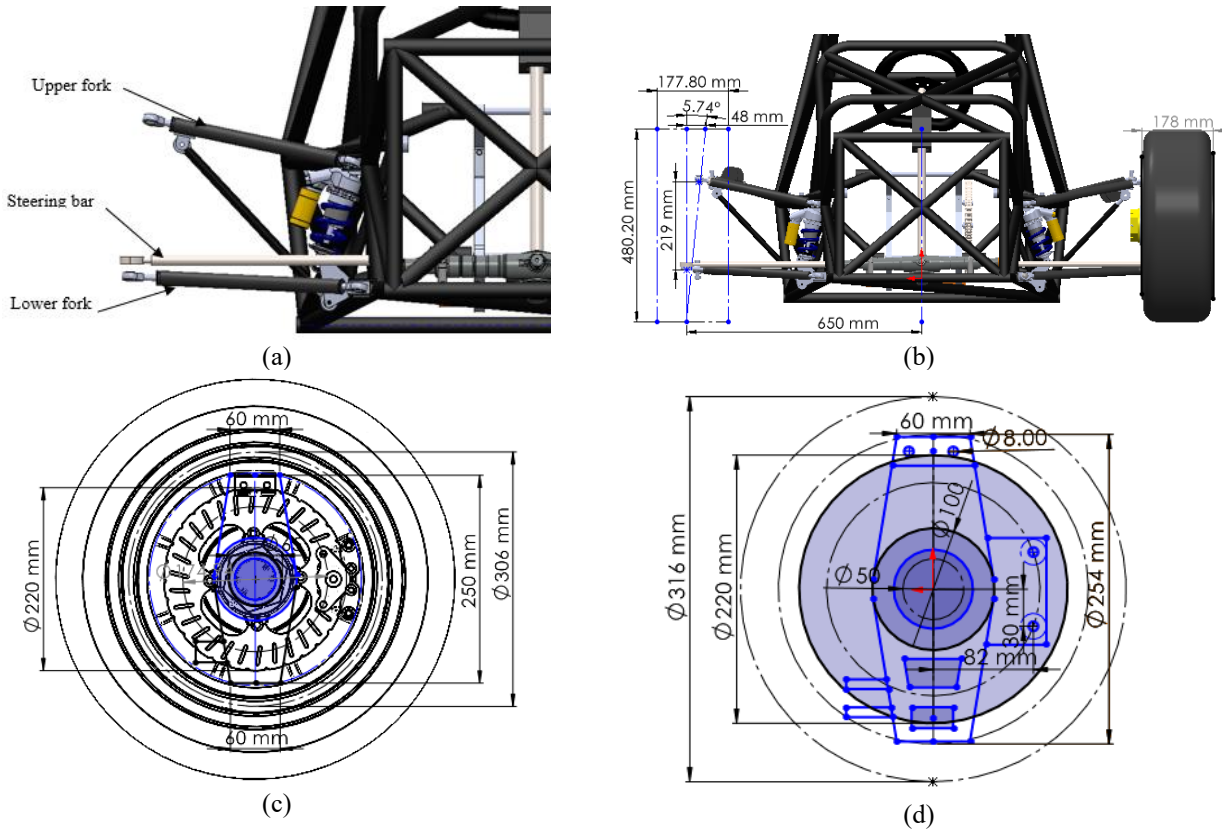

Figure 6. Front Suspension: (a) components, and (b) dimensions. Front steering knuckle: (c) base geometry for the design, and (d) initial sketch of the body's geometry

Finite element analysis was employed to generate six meshes in ANSYS with varying levels of refinement for the front steering knuckle (see Table 7). Higher refinement generally leads to more accurate results. According to Medina and Morocho [31], a solution convergence of 5% (error between results of two successive meshes) is considered acceptable, and this criterion was adopted in the present study. Furthermore, the selected mesh is used to validate the numerical model by comparing its results with simulation data from the study by Li et al. [14].

Table 7. Features of the meshes used in the independence study

Mesh	Cell size (mm)	Elements	Nodes number
1	7	21597	39282
2	3	46171	80347
3	2	88929	153396
4	1	353642	597106
5	0.5	1428002	2389538
6	0.4	2223721	3726815

2.4 Static Analysis of the Front Steering Knuckle

The static analysis of the front steering knuckle was performed using ANSYS software. Specifically, the forces acting on the front steering knuckle were configured in ANSYS. The forces generated by mass transfer during braking, cornering, and obstacle negotiation were considered. The structural parameters evaluated in the static analysis comprise Von-Mises stress, maximum deformation, and FoS. The forces acting on the front steering knuckles are as follows:

- Weight transfer and moment during break, calculated using Eqs. (6) and (9).
- Lateral weight transfer is determined using Eq. (13).
- Force generated by the steering arm, calculated using Eq. (14).
- Force exerted when overcoming an obstacle, computed using Eq. (19).

In addition to the forces, the material constituting the front steering knuckle of the racing car must also be considered. This material must withstand the stress experienced by the front steering knuckle during the operation of the FSAE vehicle. Most FSAE teams construct their knuckles using Aluminum 7075-T6, as its mechanical properties are comparable to those of Alumold Aluminum. Therefore, this work proposes the analysis of two materials: Aluminum 7075-T6 (material characteristics in Table 8), known for its lightweight properties and use in the aerospace and automotive industries, and Alumold Aluminum (see Table 9), which offers high corrosion resistance, machinability, and is used in the metalworking industry [23].

Table 8. Mechanical properties of the Aluminum 7075 T6

Properties	Values	Unit
Density	2.81	g/cm³
Tensile strength	503	MPa
Elastic limit	572	MPa
Young's modulus	72	GPa
Poisson's ratio	0.33	-
Fatigue resistance	159	MPa

Table 9. Mechanical properties of Alumold

Properties	Values	Unit
Density	2.8	g/cm³
Tensile strength	560	MPa
Elastic limit	510	MPa
Young's modulus	72	GPa
Poisson's ratio	0.33	-

2.4 Topological Optimization

Topological optimization of the front steering knuckle was performed using ANSYS and SolidWorks to reduce the mass of the initially generated front steering knuckle. Aluminum 7075-T6 and Alumold were selected for the knuckle's fabrication. Subsequently, a static analysis of the optimized geometries obtained from the TO was carried out to verify that the minimum recommended FoS of 1.5, as specified in Pang and Fard [20], was exceeded.

3. Results and Discussion

Before discussing the structural performance and optimization results, the numerical model was validated against a published benchmark case to establish confidence in its predictive capability. The validation procedure and its outcomes are presented in Section 3.2.3 and provide the foundation for the subsequent analyses.

3.1 Calculation of the Stresses at the Front Steering Knuckle Anchor Points

Table 10 summarizes all the values required for calculating the stresses on the front steering knuckle of the FSAE racing car. By inputting the values from Table 10 into Equations (1) to (19), the results in Table 11 are obtained. Table 12 highlights the load values from Table 11 applied to the front steering knuckle simulation. Li et al. [14] reported the following loads applied to the front steering knuckle: Ha = 4731.0 N, Fa=7193.8 N, H0 = 1951.8 N, Fyf=1730.1 N, and Fon_tires=1323.9 N. Their study focuses solely on cornering under braking conditions. In the present study, Ha (34.39%) and Fa (39.44%) were found to be lower, whereas H0 (25.51%), Fyf (54.99%), and Fon_tire (3.17%) were higher compared to the values reported by Li et al. [14]. Furthermore, our work utilized the FSAE 2024 regulations to select various suspension system components, ensuring that the front steering knuckle design is suitable for competition.

Table 10. Input values for calculating the stresses on the front steering knuckle

Nomenclature	Description	Unit	Magnitude
v_i	Initial velocity	Km/h	105
v_f	Final velocity	Km/h	0
t	Time	s	3
m	Mass (vehicle plus driver)	kg	360
m_v	Vehicle mass	kg	290
m_p	Driver mass	kg	70
h	CG Height	m	0.31
lt	Distance between axes	m	1.60
g	Acceleration due to gravity	m/s2	9.81
W	Weight of the vehicle including the driver	N	3531.6
k	Tire mass distribution ratio	-	0.75
m_n	Tire mass (Hoosier catalog)	kg	5
r_n	Actual tire radius	m	0.2604
μ	FSAE friction coefficient of tires	-	1.1
r_{din}	Dynamic radius (Hoosier catalog 13" rim)	m	0.3302
l_2	Front axle distance to CG	m	0.965
v_x	Vehicle velocity in x	km/h	48

Table 10. Continued

Nomenclature	Description	Unit	Magnitude
r	Tightest curve radius	m	11.5
T_d	Front track width	m	1.35
θ	Tilt angle	degrees	20
v_1	Vehicle velocity on the curve	km/h	10
r_1	Curvature radius	m	4.5
$\emptyset$	Bolt diameter	m	0.008
S_r	Strong section	m	0.0081
e	Thickness	m	0.003
β	Obstacle angle	degrees	30
v_{y2}	Vehicle final velocity in y	km/h	0
h_1	Obstacle height	cm	10
R_{rd}	Front wheel mass distribution	%	30

Table 11. Results from Eqs. (1) to (19)

Nomenclature	Description	Unit	Magnitude	Equation
a	Acceleration	m/s2	9.72	(1)
ΔF_a	Longitudinal mass transfer	N	678.13	(2)
C_{tv}	Total vertical load	N	4209.73	(3)
I_n	Tire inertia	kg.m2	0.25	(4)
F_b	Normal force at point B	N	1431.92	(5)
F_a	Normal force at point A	N	2099.68	(6)
H_a	Friction force at point A	N	2309.65	(7)
H_b	Friction force at point B	N	1190.35	(8)
M_f	Braking moment	Nm	381.32	(9)
$F_{centrifugal}$	Centrifugal force	N	5565.22	(10)
$A_{centrifugal}$	Centrifugal acceleration	m/s2	15.46	(11)
F_0	Increased load on front axle	N	3124.24	(12)
H_0	Front tire lateral load in cornering	N	3288.92	(13)
F_{yf}	Lateral force on the front axle	N	5956.79	(14)
τ_p	Bolt shear stress	MPa	32.71	(15)
τ_c	Shear stress at point C	MPa	33.84	(16)
v_y	Vertical velocity	km/h	27.71	(17)
a_y	Vertical acceleration	m/s2	296.30	(18)
F_{on_tires}	Force on tires overcoming an obstacle	N	20878.35	(19)

Table 12. Loads applied to the front steering knuckle simulation

Nomenclature	Description	Unit	Magnitude
H_a	Friction force at point A	N	2309.65
F_a	Normal force at point A	N	3124.24
H_0	Front tire lateral load in cornering	N	3288.92
F_{yf}	Lateral force on the front axle	N	5956.79
F_{on_tires}	Force on tires overcoming an obstacle	N	20878.35

3.2 Front Steering Knuckle Design

Figure 7(a) shows the initial design of the front steering knuckle. This design considers the knuckle's caster angle and anchoring points, appropriately positioning the steering supports, suspension upright supports (upper and lower), and the brake caliper support. Additionally, it incorporates the wheel hub, which houses the bearing, brake disc, and wheel. The initial knuckle is made of Aluminum 7075-T6 with a mass of 2.41 kg. By comparing the errors between meshes for maximum von Mises stress, maximum deformation, and minimum FoS (see Table 13), Mesh 4 was selected. Mesh 4 was chosen because its errors are 2% lower than those of Mesh 5. The Mesh 4 (331,960 elements) ensures results with good

precision while maintaining an acceptable computational cost. The details of Mesh 4 are illustrated in Figure 7(b). In addition to ensuring numerical convergence, the selected mesh configuration forms the basis of the validation strategy adopted in this study. The converged mesh is subsequently employed to reproduce a reference case reported in the literature, allowing the numerical model to be assessed against independent published results. To assess the reliability and predictive capability of the numerical model developed in this study, a validation procedure based on comparison with published reference data was carried out. Given the absence of publicly available experimental measurements with sufficient geometric detail for front steering knuckles under Formula SAE conditions, a numerical cross-validation approach was adopted. The validation case corresponds to the optimized front steering knuckle geometry reported by Li et al. [14], which represents a widely cited benchmark in the structural optimization of Formula SAE components. The same material (Aluminum 7075-T6), loading conditions associated with emergency cornering, and boundary conditions described in Li et al. [14] were reproduced as closely as possible.

Table 13. Results of the mesh independence study

Mesh	Cell size (mm)	Elements	Maximum von-Mises (MPa)	Error (%)	Maximum deformation (mm)	Error (%)	Minimum FoS	Error (%)
1	7	21597	161.21	2.874	0.067031	0.643	2.7517	1.994
2	3	46171	165.98	0.294	0.067465	0.354	2.6979	0.041
3	2	88929	166.47	6.844	0.067705	0.252	2.6990	8.233
4	1	353642	178.70	0.590	0.067876	0.087	2.4937	0.435
5	0.5	1'428002	179.76	0.663	0.067935	0.007	2.4829	0.984
6	0.4	2'223721	180.96	-	0.067940	-	2.4587	-

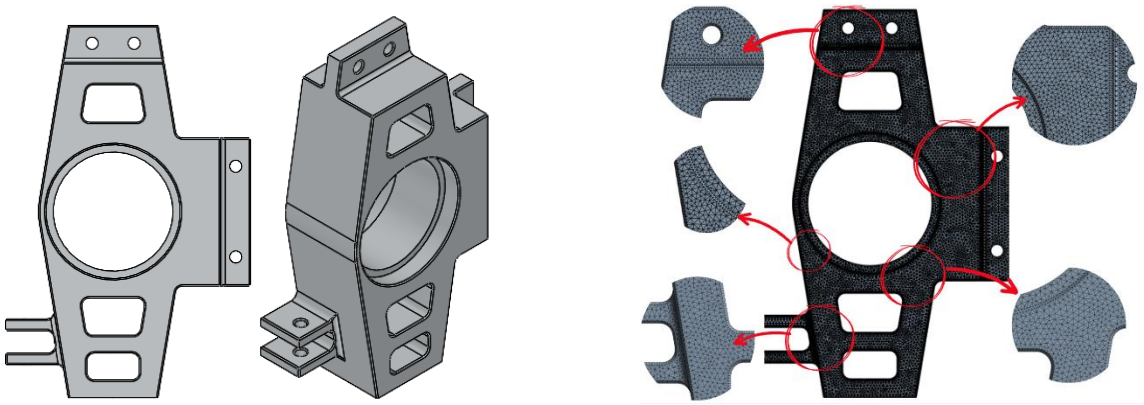

(a) (b)

Figure 7. Front steering knuckle: (a) CAD design, and (b) Mesh 4

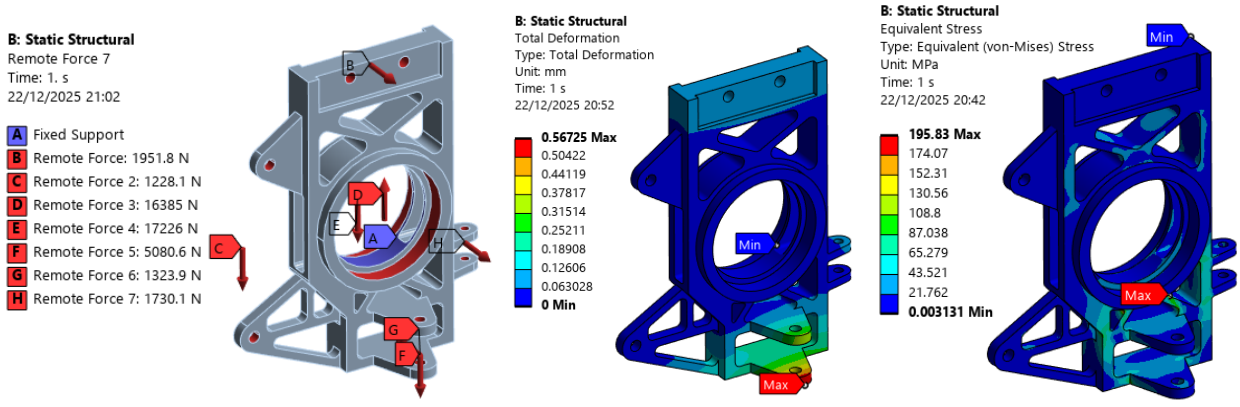

(a) (b) (c)

Figure 8. Front steering knuckle employed in the validation stage: (a) applied loads, (b) maximum total deformation, and (c) maximum equivalent stress (Von-Mises)

The finite element discretization employed for the validation analysis corresponds to Mesh 4, previously selected through the mesh independence study presented. This ensures that numerical discrepancies are not influenced by mesh density effects. Figures 8(b) and 8(c) show the resulting deformation field and equivalent Von Mises stress distribution obtained in the present work. The maximum total deformation and maximum equivalent stress were found to be 0.56725

mm and 195.83 MPa, respectively. These values differ by only 1.55% and 1.87% from those reported by Li et al. [14], who obtained 0.5586 mm and 199.57 MPa. The close agreement between both sets of results provides confidence in the accuracy of the numerical modeling strategy, including load application, boundary conditions, material modeling, and mesh selection. Although direct experimental validation could not be performed due to insufficient geometric information in the available experimental literature, the adopted numerical cross-validation approach is considered appropriate and robust for the objectives of the present study.

3.2 Static Analysis of the Initial Front Steering Knuckle

For this analysis, the most critical scenario was considered, in which the vehicle negotiates a curve and generates braking torque while overcoming an obstacle. Figure 9 details the loads applied to the knuckle geometry. The applied load values are specified in Table 12. Figure 10 presents the results obtained using ANSYS software for the front steering knuckle made of Aluminum 7075-T6. It shows the total deformation, maximum Von-Mises stress, directional deformation along the y-axis, and the FoS. The maximum total deformation observed is 0.067876 mm, while the maximum equivalent Von-Mises stress reaches 178.7 MPa. The maximum directional deformation along the y-axis resulted in 0.041346 mm, and the minimum FoS, located at the lower part of the front steering knuckle, resulted in 2.4937. Pang and Fard obtained a total deformation of 0.00304 mm, a maximum equivalent stress of 239.3 MPa, and a minimum FoS of 1.55 [20]. Their results are similar to the present study due to the same material and comparable design constraints. Furthermore, comparing the FoS obtained by Pang and Fard [20], there is room to reduce the FoS while maintaining the structural rigidity required for FSAE competitions.

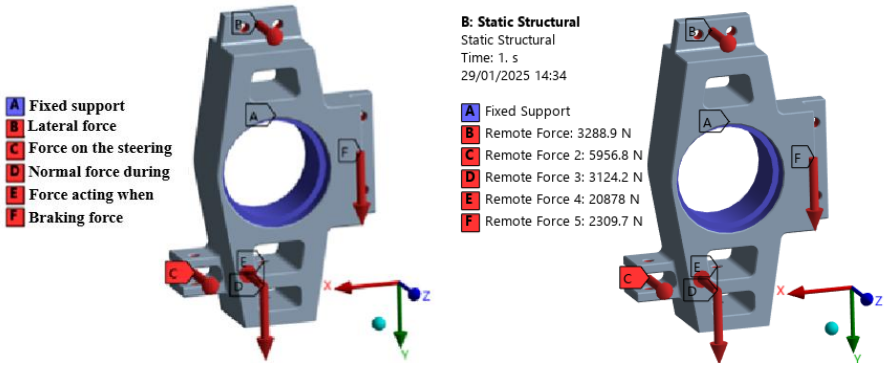

(a) (b)

Figure 9. Application of loads on the front knuckle: (a) boundary conditions, and (b) loads

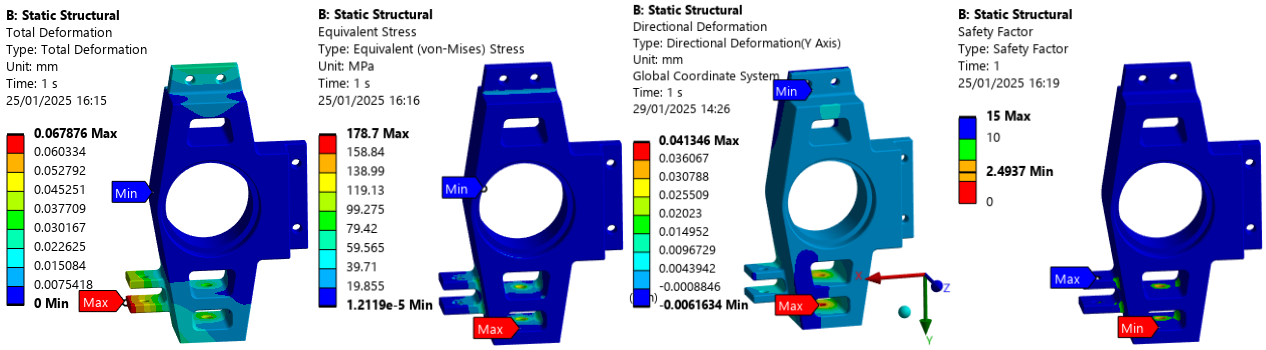

(a) (b) (c) (d)

Figure 10. Structural parameters in the front steering knuckle made of 7075-T6 Aluminum: (a) maximum total deformation, (b) maximum equivalent stress (Von-Mises), (c) directional deformation in "y" axis, and (d) FoS

Figure 10 shows that the lower part of the knuckle reaches the maximum total deformation (0.067876 mm), specifically in the steering rod attachment. According to Bhardwaj et al. [8], Li et al. [14], Gupta et al. [15], and Kothari et al. [18], the deformation is also concentrated in this area. Additionally, the results obtained by Anitha and Shankar [5] are similar to those of this work, validating that the maximum total deformation values do not compromise the knuckle design. The lower part of the front steering knuckle reaches the maximum equivalent stress, specifically in the lower support. Results confirm that the area in the steering road attachment is the most critical. Since this area bears the highest loads, as also found by [10, 14, 20, 23]. Remarkably, in this work, the maximum stress does not exceed the permissible limit of 336.66 MPa, ensuring structural safety due to the selection of Aluminum 7075-T6. The minimum FoS of 1.5 is within acceptable limits according to the established design criteria, as evidenced by the works of Bhardwaj et al. [8] and Pang and Fard [20], who used this criterion. Similarly, the maximum deformation value does not affect the suspension system's performance, reinforcing the design's validity. The front knuckle design maintains an adequate FoS because results resemble previous works [4,7, 9, 11-12, 15, 17, 23, 31]. Note that [5, 7, 9, 12] reported Von-Mises stresses below

100 MPa using mild steel as the base material. In contrast, the study by Agarwal and Saatyaki [16] reported an equivalent Von-Mises stress of 408 MPa, exceeding the permissible stress of 336.66 MPa.

The static analysis performed in ANSYS on the knuckle made of Alumold (see Figure 11) identifies the areas of maximum deformation. The total deformation reaches a maximum of 0.06774 mm, represented in red. These areas coincide with the points of highest load concentration and are crucial for evaluating the structural integrity of the component. The maximum equivalent Von-Mises stress is 202.6 MPa. The maximum directional deformation along the y-axis is 0.040852 mm. The FoS analysis revealed critical zones marked in orange, which are particularly vulnerable to failure due to their low values. The analysis reports a FoS of 2.3112. The values obtained in this work for Alumold are close to those of Pang and Fard [20], as the design constraints are similar, despite their use of Aluminum 7075-T6. Furthermore, comparing the FoS obtained in this study with other works, there is room to reduce the FoS while maintaining the structural rigidity required for FSAE competitions, thereby reducing the amount of material in the front steering knuckle. As shown in Figure 11, the maximum total deformation (0.040852 mm) is located at the lower part of the knuckle, particularly where the steering rod is connected. According to [8, 14-15, 18], deformation is also concentrated in this area. Additionally, the results achieved by Bhardwaj et al. [8] are analogous to those found in this study, concluding that the total deformation values do not compromise the knuckle steering design. The maximum equivalent Von-Mises stress is located at the lower part of the knuckle, where the lower support is situated. This confirms that the region where the steering rod is attached is critical to the design, as it bears the highest loads, as also noted by [10, 14, 20, 23]. However, due to the selection of Alumold, the maximum stress does not exceed the permissible limit of 230 MPa, ensuring the structural safety of the knuckle. Similarly, for Alumold, the minimum FoS is within acceptable limits.

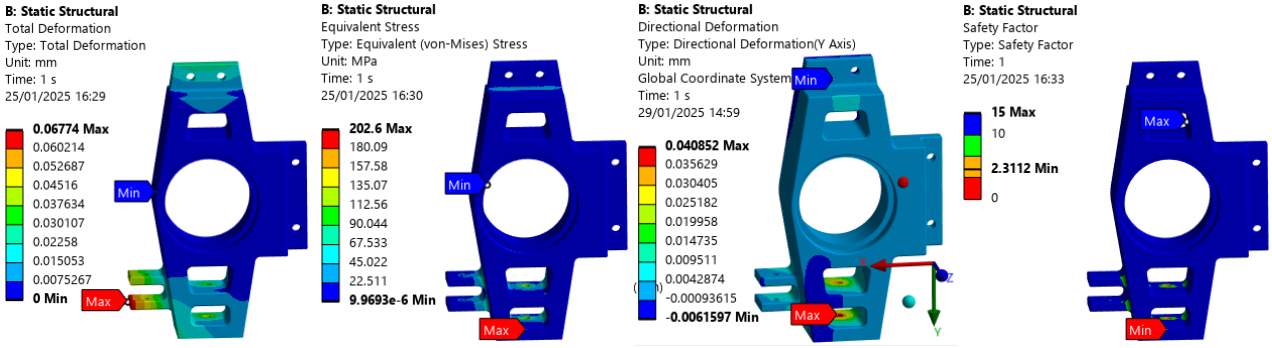

(a) (b) (c) (d)

Figure 11. Structural parameters in the front steering knuckle made of Alumold: (a) maximum total deformation, (b) maximum equivalent stress (Von-Mises), (c) directional deformation in the "y" axis, and (d) FoS

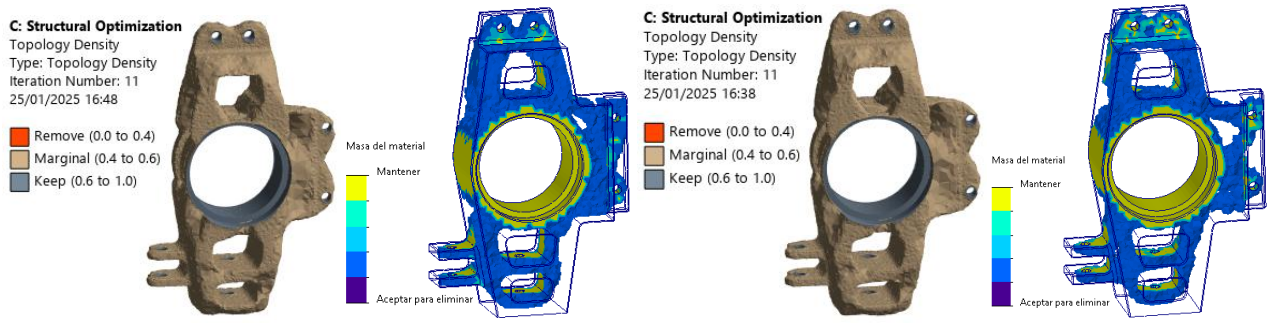

(a) (b) (c) (d)

Figure 12. Optimized front steering knuckles: (a) 7075 T6 Aluminum - ANSYS, (b) 7075 T6 Aluminum - SolidWorks, (c) Alumold Aluminum - ANSYS, and (d) Alumold Aluminum - SolidWorks

3.3 Topology Optimization of the Front Steering Knuckle

Based on the results obtained from the simulation of the initial knuckle, its geometry is optimized to reduce mass while maintaining a minimum FoS of 1.5. Figure 12 shows the results of the TO of the knuckle, performed using ANSYS and SolidWorks software, with Aluminum 7075-T6 and Alumold as materials. The total mass removed using ANSYS was 35% for both materials, resulting in optimized masses of 1.34 kg for Aluminum 7075-T6 and 1.40 kg for Alumold. On the other hand, SolidWorks achieved a 25% reduction in the initial knuckle mass, yielding optimized masses of 1.31 kg for Aluminum 7075-T6 and 1.33 kg for Alumold. It is worth noting that the initial mass of the front knuckle was 2.41 kg. In the optimization performed with ANSYS (see Figure 12), the grey areas cannot be removed due to constraints imposed by the loading conditions. In contrast, the orange areas were removed, while the brown areas indicate where material has been retained. For the optimization in SolidWorks (see Figure 12), the constrained zones are highlighted in yellow and must be preserved, while the blue areas indicate removed material. Notably, the material removal in SolidWorks is more

pronounced in the lower section compared to the upper section. The optimized geometry in SolidWorks differs from that obtained with ANSYS.

In the additive manufacturing process, a metal 3D printer is used for part production. Additive manufacturing enables the creation of complex geometries that would not be feasible through machining, making it ideal for TO. On the other hand, machining allows for the adjustment and adaptation of various geometries, ensuring their viability for fabrication using CNC (Computer Numerical Control) machines. In the Peruvian market, metal 3D printers are not commercially available, and their import cost is high. Therefore, in this work, the decision was made to proceed with CNC machining after TO. The CNC machining process is widely used in Peru. Consequently, after performing TO, the geometries of the front steering knuckle are prepared for CNC machining. Figure 13 shows the modified geometry for machining the front knuckle, derived from the TO results obtained using ANSYS and SolidWorks.

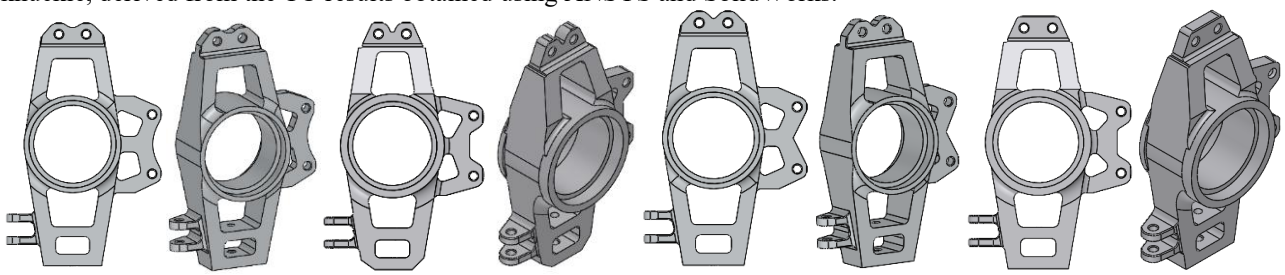

(a) (b) (c) (d)

Figure 13. Optimized front steering knuckle geometry for machining: (a) 7075 T6 Aluminum - ANSYS, (b) 7075 T6 Aluminum - SolidWorks, (c) Alumold Aluminum - ANSYS, and (d) Alumold Aluminum - SolidWorks

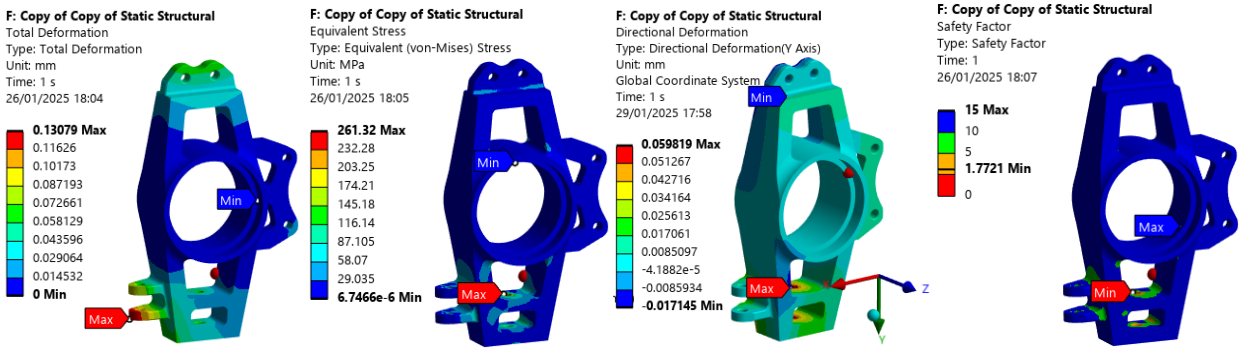

(a) (b) (c) (d)

Figure 14. Optimized front steering knuckle in ANSYS for machining (Aluminum 7075-T6): (a) maximum total deformation, (b) maximum equivalent stress (Von-Mises), (c) directional deformation in "y" axis, and (d) FoS

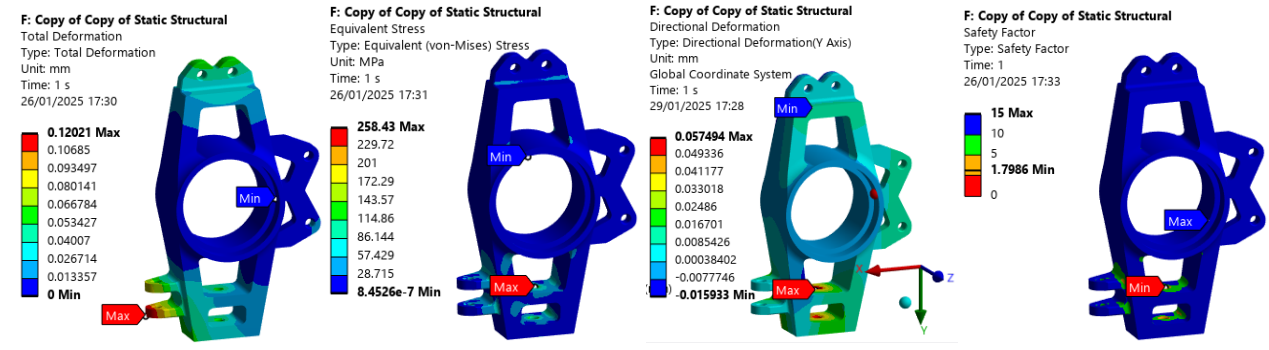

(a) (b) (c) (d)

Figure 15. Optimized front steering knuckle in ANSYS for machining (Alumold Aluminum): (a) maximum total deformation, (b) maximum equivalent stress (Von-Mises), (c) directional deformation in "y" axis, and (d) FoS

Subsequently, geometry finalization, static structural analyses were conducted using ANSYS software for the initial designs and SolidWorks for the machining-optimized front steering knuckles. For the ANSYS simulations (Figure 14), Aluminum 7075-T6 yielded a maximum total deformation of 0.13079 mm, a Von-Mises stress of 261.32 MPa, a y-axis directional deformation of 0.0059819 mm, and a minimum FoS of 1.7721, while Alumold (Figure 15) produced comparatively lower deformation at 0.12021 mm, a Von-Mises stress of 258.43 MPa, a y-axis deformation of 0.0057494 mm, and a slightly higher FoS of 1.80. For the machining-optimized geometries analyzed in SolidWorks, Aluminum 7075-T6 (Figure 16) returned a maximum total deformation of 0.18138 mm, a Von-Mises stress of 253.78 MPa, a y-axis deformation of 0.0054537 mm, and an FoS of 1.83, whereas Alumold (Figure 17) exhibited a marginally higher

deformation of 0.1836 mm, a Von-Mises stress of 286.41 MPa, a y-axis deformation of 0.0055548 mm, and an FoS of 1.63. All four design-material combinations satisfy the minimum FoS threshold of 1.5, confirming the structural integrity of both knuckle geometries across both materials. The machining-optimized designs demonstrate slightly higher deformations but remain well within acceptable limits, with Alumold consistently achieving competitive or superior safety margins. These results collectively validate the suitability of both materials for the front steering knuckle application under the prescribed loading conditions.

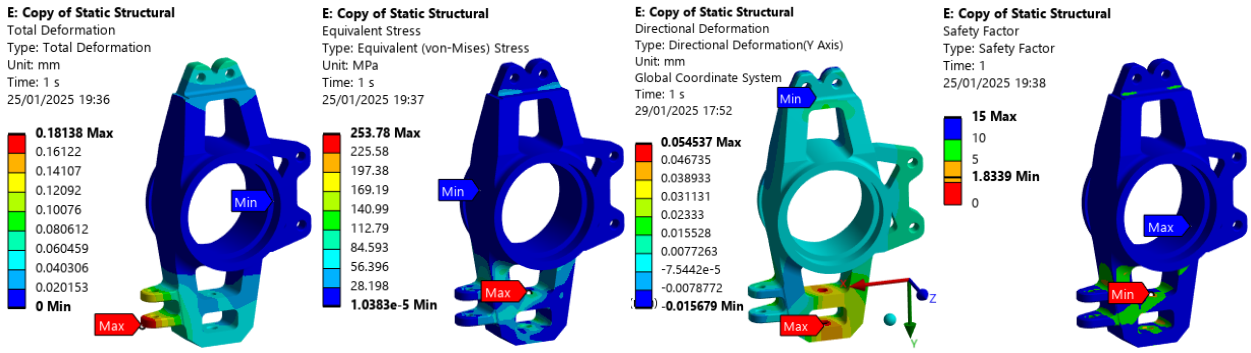

(a) (b) (c) (d)

Figure 16. Optimized front steering knuckle in SolidWorks for machining (Aluminum 7075-T6): (a) maximum total deformation, (b) maximum equivalent stress (Von-Mises), (c) directional deformation in "y" axis, and (d) FoS

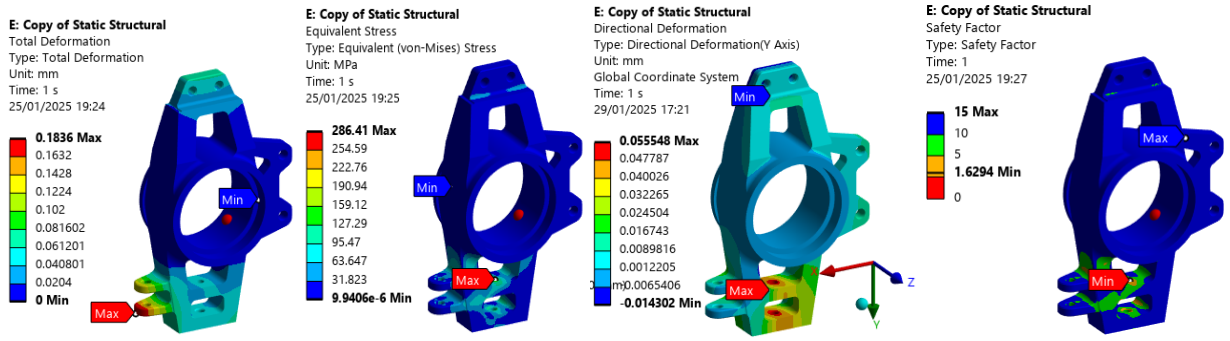

(a) (b) (c) (d)

Figure 17. Optimized front steering knuckle in SolidWorks for machining (Alumold Aluminum): (a) maximum total deformation, (b) maximum equivalent stress (Von-Mises), (c) directional deformation in "y" axis, and (d) FoS

Finally, Table 14 summarizes the results of the masses and FoS of the initial and optimized geometries (for machining) of the front steering knuckle. In this work, the mass of the Aluminum 7075-T6 knuckle (see Table 14) was reduced to 1.31 kg. The Aluminum 7075-T6 knuckle achieved a minimum FoS of 1.83 using SolidWorks, which yielded better results than ANSYS. For the Alumold knuckle, the mass was reduced to 1.33 kg, with a FoS of 1.62, using SolidWorks. The results demonstrate that both materials (Aluminum 7075-T6 and Alumold) are suitable for designing the front steering knuckle, because their FoS exceeded the threshold of 1.5. The works of [2. 4,6-7] reduced the mass of the front steering knuckle by 50% to 60% using TO. The work of Dumbre et al. [3] reduced the initial mass of the front steering knuckle by 55% by using cast aluminum. Since the materials used in these studies exhibit lower mechanical strength than the present analysis, they achieved greater percentage reductions in the knuckle's initial mass.

Table 14. Comparison of the results of the initial and optimized spindles (for machining)

Material	Initial mass (kg)	Remaining mass %	Minimum (initial) FoS	Mass after optimization (kg)	Minimum FoS (final)
ANSYS Software					
7075 T6 Aluminum	2.41	65%	2.49	1.34	1.77
Alumold	2.41	65%	2.31	1.40	1.79
SolidWorks Software					
7075 T6 Aluminum	2.41	75%	2.49	1.31	1.83
Alumold	2.41	75%	2.31	1.33	1.62

Additionally, Figures 18 and 19 present the structural analyses of the knuckle support under lateral force loads, modeled with Aluminum 7075-T6 (32.45 g) and Alumold (32.45 g), respectively. The Aluminum 7075-T6 results show

that the maximum total deformation was 0.22335 mm (see Figure 18), in the upper part of the support (in red). The maximum equivalent Von-Mises stress reached 283.49 MPa, situated near the support's holes. The maximum directional deformation along the y-axis is 0.098037 mm, particularly in the lower hole. Finally, the minimum FoS reached 1.6607, which meets the threshold of 1.5 recommended by Pang and Fard [20] and ensures no failure under the specified load conditions. Furthermore, the maximum deformation does not affect the suspension performance, validating the design. The results of the static analysis of Alumold support are shown in Figure 19. The results indicate that the maximum total deformation is 0.22335 mm, in the upper part of the support. The maximum equivalent Von-Mises stress reached 283.49 MPa. Additionally, the maximum directional deformation along the y-axis reached 0.098037 mm. The FoS obtained was 1.6838. Note that the structural results for both supports (made of Aluminum 7075-T6 and Alumold) are quite similar.

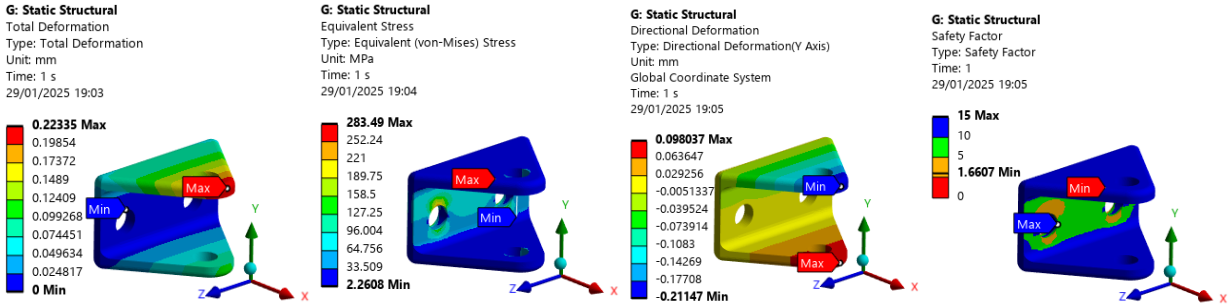

(a) (b) (c) (d)

Figure 18. Front steering knuckle support (7075-T6 Aluminum): (a) maximum total deformation, (b) maximum equivalent stress (Von-Mises), (c) directional deformation in "y" axis, and (d) FoS

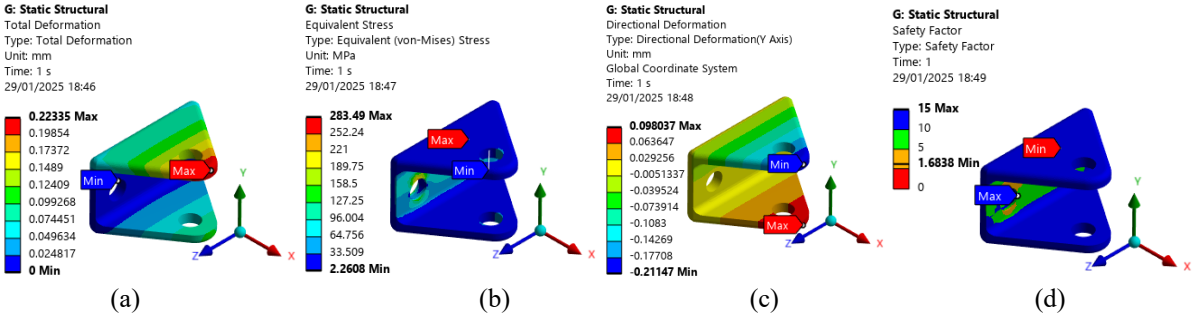

(a) (b) (c) (d)

Figure 19. Front steering knuckle support (Alumold Aluminum): (a) maximum total deformation, (b) maximum equivalent stress (Von-Mises), (c) directional deformation in "y" axis, and (d) FoS

Figure 20 shows the final geometries (finished product) of the front steering knuckles for CNC machining, assembled with their support. Additionally, the materials used for the front knuckle and CNC machining were quoted in the Peruvian market. The prices for Aluminum 7075-T6 and Alumold plates, with dimensions of 290 mm x 167 mm x 70 mm, are $167.11 and $193.80, respectively. As for CNC machining, the service excluding VAT costs $107.81. These low prices and accessibility demonstrate that the Aluminum 7075-T6 is the best material for constructing the front knuckle of the racing car. Designing results showed that the Aluminum 7075-T6 exhibits superior technical characteristics (lower mass), and economic advantages (lower cost) compared to Alumold.

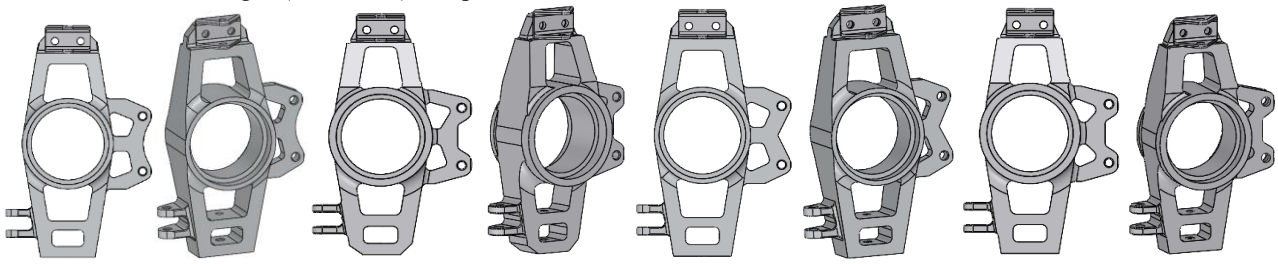

(a) (b) (c) (d)

Figure 20. Optimized front knuckle geometry and bracket assembly: (a) 7075 T6 Aluminum - ANSYS, (b) 7075 T6 Aluminum - SolidWorks, (c) Alumold Aluminum - ANSYS, and (d) Alumold Aluminum - SolidWorks

Table 15 compares the main characteristics of 7075-T6 and Alumold aluminum, both considered for the manufacture of the front knuckle. Although both have similar mechanical strength (approximately 510-540 MPa), Alumold offers superior machinability, which facilitates manufacturing processes and improves the quality of the surface finish. However, this advantage implies a higher cost per kilogram compared to 7075-T6 aluminum. Therefore, the choice between these alloys depends on the balance between performance requirements and production costs. Table 16 compares

the optimization capabilities of ANSYS and SolidWorks. ANSYS enables more precise control in topology optimization, achieving greater weight reductions (30-60%) at the cost of longer simulation times, making it better suited to advanced engineering design. In contrast, SolidWorks offers faster results on simple models (10-30% reduction), making it ideal for preliminary design or rapid prototyping stages.

Table 15. Comparison of the characteristics of 7075-T6 Aluminum and Alumold

Characteristic	Aluminum 7075-T6	Alumold
Alloy type	Series 7000 (Zn)	Series 7000 or 5000 (depending on the type)
Heat treatment	T6 (thermal solution + aging)	Normally precipitated and thermally stabilized
Mechanical resistance	Very high (510-538 MPa)	High (510-540 MPa)
Machinability	Good	Excellent
Applications	Aerospace, structures, automotive	Plastic injection molds, blow molds
Cost per kilo	$ 41.75	$ 48.56

Table 16. Comparison of ANSYS and SolidWorks software features

Characteristics	ANSYS	SolidWorks
Weight reduction achievement	30-60% with more precise control.	10-30% in simple models.
Simulation time	Long (depending on the model and complexity), on average 12 minutes.	Short in simple models. Average 5 minutes.
Final design quality	Ideal for final design, especially in advanced engineering.	Suitable for preliminary design or prototype.

4. Conclusions

The front steering knuckle structure of a Formula SAE racing car was optimized to reduce its weight. Initially, the stresses at the anchoring points were determined considering the suspension geometry and Formula SAE regulations, including braking conditions, normal forces during acceleration, lateral forces during cornering, stresses generated by the steering joint, and loads applied when overcoming an obstacle. The analysis yielded a front braking force of 2309.65 N, a normal braking force of 3124.24 N, a lateral cornering force of 3288.92 N, a steering joint force of 5956.79 N, and a force required to overcome an obstacle of 20878.35 N. The front knuckle of the Formula SAE racing car was designed and modeled in SolidWorks, considering the dimensions of the steering rack, tire, rim, brake disc, brake caliper, wheel hub, and bearings. This initial design underwent a static analysis to calculate the maximum Von Mises stress, total displacement, and FoS of the front steering knuckle. Finally, TO was performed on the front knuckle to reduce its weight. The anchoring points and applied loads were considered in the optimization, resulting in a 35% reduction in the knuckle's mass using ANSYS software. The resulting masses were 1.34 kg for Aluminum 7075-T6 and 1.40 kg for Alumold. On the other hand, using SolidWorks, the mass reduction was 25%, yielding masses of 1.31 kg for Aluminum 7075-T6 and 1.33 kg for Alumold. The optimization results maintained the knuckle's FoS above 1.5. In future research, we recommend focusing the steering knuckle design on advanced manufacturing, incorporating additive manufacturing technologies, particularly metal 3D printing. This approach would optimize the structural efficiency of the component, leveraging the technology's advantages, such as weight reduction, design freedom for complex geometries, and the integration of functions impractical with conventional manufacturing processes.

Acknowledgements

The authors thank everyone involved in this study, particularly those who provided the facilities that made this work possible.

Funding

This study was not supported by any grants from funding bodies in the public, private, or not-for-profit sectors.

Declaration of Competing Interest

The author declares no conflicts of interest.

CRediT Authorship Contribution Statement

A.R. Ramírez (Methodology; Software; Formal analysis;)
C.E. Yactayo (Methodology; Formal analysis; Writing - original draft)
C.V. Rodriguez (Conceptualisation; Investigation; Supervision; Writing - review & editing)
D.D. De La Torre (Software; Writing - review & editing)

Availability of Data and Materials

The data supporting this study's findings are available on request from the corresponding author.

Ethics Declarations
This study did not involve human participants or animals. Ethical approval was therefore not required.

Generative Artificial Intelligence Declarations
The authors stated that generative AI was not used to generate content, ideas, or theories. We have just utilized AI to enhance readability and refine the language. This was used with extreme human control and oversight. The authors take full responsibility for reviewing and approving the content.

References
[1] A. Anthony, "FSAE vehicle instrumentation and validation," Honors thesis, Western Michigan University, 2022. [Online]. Available: https://scholarworks.wmich.edu/honors_theses/3500

[2] S. S. Kaldhone and S. U. Sapkal, "Product re-engineering by topology optimization for forged component," *International Journal of Emerging Trends in Engineering Research*, vol. 9, no. 9, pp. 1266–1270, 2021.

[3] P. Dumbre, A. Mishra, V. Aher, and S. Swapnil, "Structural Analysis of steering Knuckle for Weight Reduction," *International Journal of Emerging Technology and Advanced Engineering*, vol. 4, no. 6, pp. 552-557, 2014.

[4] G. Y. Kim, S. H. Han, and K. H. Lee, "Structural optimization of a knuckle with consideration of stiffness and durability requirements," *The Scientific World Journal*, vol. 2014, p. 763692, 2014.

[5] P. Anitha and V. Hari Shankar, "Design and topology optimisation of a steering knuckle joint using FEA," *International Journal of Scientific and Research Publications*, vol. 6, no. 11, pp. 311–316, Nov. 2016.

[6] V. Shaisundaram, L. Karikalan, V. Vignesh, R. Tamilmani, and A. Mushfiqur, "Design and analysis of steering knuckle component for terrain vehicle," *International Journal of Recent Trends in Engineering and Research*, vol. 4, no. 3, pp. 36–42, Mar. 2018.

[7] A. Bhusari, A. Chavan, and S. Karmarkar, "FEA & optimisation of steering knuckle of ATV," in *40th IRF International Conference*, Pune, India, 2016, pp. 51–56.

[8] S. Bhardwaj, B. Ashok, U. Lath, and A. Agarwal, "Design and optimization of steering upright to reduce the weight using FEA," SAE Technical Paper 2018-28-0081, Jul. 2018.

[9] S. V. Dusane, M. K. Dipke, and M. A. Kumbhalkar, "Analysis of steering knuckle of all terrain vehicles (ATV) using finite element analysis," *IOP Conference Series: Materials Science and Engineering*, vol. 149, no. 1, p. 012133, Sep. 2016

[10] L. Rajeshkumar, V. Bhuvaneswari, B. Pradeepraj, M. Praveen Pauldurai, C. Palanivel, and S. Sandeep Kumar, "Design and optimization of static characteristics for a steering system in an ATV," *IOP Conference Series: Materials Science and Engineering*, vol. 954, no. 1, p. 012009, 2020.

[11] M. Shuaib, A. Haleem, L. Kumar, Rohan, and D. Sharma, "Design and analysis of steering knuckle joint," in *Advances in Engineering Design: Select Proceedings of FLAME 2018*, Singapore: Springer, 2019, pp. 423–431.

[12] B. A. Saputro et al., "Static load simulation of steering knuckle for a formula student race car," *AIP Conference Proceedings*, vol. 1931, no. 1, p. 030049, 2018.

[13] S. Yadav, R. K. Mishra, V. Ansari, and S. B. Lal, "Design and analysis of steering knuckle component," *International Journal of Engineering Research and Technology*, vol. 5, no. 4, pp. 457–463, Apr. 2016.

[14] J. Li, J. Tan, and J. Dong, "Lightweight design of front suspension upright of electric formula car based on topology optimization method," *World Electric Vehicle Journal*, vol. 11, no. 1, p. 15, Feb. 2020.

[15] H. Gupta and N. K. Singh, "Design and analysis of steering knuckle of hybrid metal matrix composite for the FSAE vehicle," *Materials Today: Proceedings*, vol. 46, pp. 10551–10557, 2021.

[16] S. Agarwal and T. Saatyaki, "Fatigue analysis for upright of a FSAE vehicle," *International Journal of Engineering Research and Technology*, vol. 9, no. 3, pp. 413–416, Mar. 2020.

[17] A. Hasan, C. Lu, and W. Liu, "Lightweight design and analysis of steering knuckle of formula student car using topology optimization method," *World Electric Vehicle Journal*, vol. 14, no. 9, p. 233, Aug. 2023.

[18] P. Kothari, E. Dias, and S. Chaphale, "Design and fatigue analysis of upright on FSAE vehicle," *International Research Journal of Engineering and Technology*, vol. 8, no. 8, pp. 1105–1113, Aug. 2021.

[19] J. Mesicek, M. Pagac, J. Petru, P. Novak, J. Hajnys, and K. Kutiova, "Topological optimization of the formula student bell crank," *MM Science Journal*, vol. 2019, no. 3, pp. 2964–2968, Oct. 2019.

[20] T. Y. Pang and M. Fard, "Reverse engineering and topology optimization for weight-reduction of a bell-crank," *Applied Sciences*, vol. 10, no. 23, p. 8568, Nov. 2020.

[21] P. V. Wable and S. S. Shah, "Design analysis & optimization of hub used in FSAE cars," *International Journal of Innovative Research in Science, Engineering and Technology*, vol. 6, no. 8, pp. 16799–16808, Aug. 2017.

[22] SAE International, *Formula SAE Rules 2024*, ver. 1.0, Sept. 1, 2023. [Online]. Available: https://www.fsaeonline.com/cdsweb/gen/DownloadDocument.aspx?DocumentID=369d01c0-589d-4ebe-b8d4-b07544f4a52b

[23] C. A. Padilla-Padilla, E. Pozo-Safla, F. Ballin-Juna, and D. Herrera-Santamaría, "*Optimización topológica de las manguetas delanteras y posteriores para un vehículo prototipo fórmula SAE*," Dominio de las Ciencias, vol. 6, no. 3, pp. 984–1005, 2020.

[24] KAZ Technologies, "Steering Rack." Accessed: Jan. 02, 2025. [Online]. Available:

https://www.kaztechnologies.com/steering-rack
[25] Hoosier Racing Tire, "Formula Student SAE." Accessed: Jan. 02, 2025. [Online]. Available: https://hoosiertiregp.com/20-5x7-0-13-r20/
[26] OZ Racing, "Formula Student." Accessed: Jan. 02, 2025. [Online]. Available: https://www.ozracing.com/motorsport/formula-student/wheels
[27] NG Brakes, "Main page." Accessed: Jan. 02, 2025. [Online]. Available: https://ngbrakes.com/
[28] Wilwood Engineering, "GP200 Caliper Calipers." [Online]. Available: https://www.wilwood.com/Calipers/CaliperList?subname=GP200 Caliper
[29] C. Valdeolmillos, "Diseño del buje monotuerca para un monoplaza de Fórmula SAE," Escuela Técnica Superior de Ingenieros Industriales, 2023. [Online]. Available: https://oa.upm.es/72572/1/tfg_carlos_manuel_valdeolmillos_carnicero.pdf
[30] SKF, "Main page." Accessed: Jan. 02, 2025. [Online]. Available: https://www.skf.com/pe
[31] W. Medina and J. Morocho, "Diseño y construcción de manguetas y cubos de rueda de un vehículo de competencia Fórmula SAE eléctrico," Universidad Politécnica Salesiana Sede Matriz Cuenca. [Online]. Available: https://dspace.ups.edu.ec/bitstream/123456789/15056/1/UPS-CT007433.pdf